Non-contact structure solar desalination system for higher depths

Matta Uday Kiran[1], *Ajay* Kumar Kaviti[1,2*]

[1]Department of Mechanical Engineering, VNRVJIET, Hyderabad, Telangana, India.
[2]Centre for Solar Energy Materials, VNRVJIET, Hyderabad, Telangana, India.

Abstract. To address the worldwide issue of water scarcity, prompt action is required. Solar desalination is one potential sustainable solution that could be considered for this problem. A nano-structure solar still that does not require touch is the subject of this investigation. As a result of the non-contact structure, the solar still structure does not meet water, which not only extends its lifespan but also prevents salt from accumulating when it is doing continuous operation. One side of the non-contact structure is made to be a high absorber of sun's light, while the other side is made to be a high emitter of the infrared wavelength. A total of three and four centimeters of saline water were used in the experiments that were conducted. The information was gathered over the course of three months to evaluate the performance of the construction in a variety of specific environmental conditions. Several characteristics, such as glass, basin, vapor, water, absorber, ambient temperature, time, and solar intensity, were measured over the course of the experiment. In proportion to the increasing water depth, the NCNS system generates a greater quantity of distillate than the CSS system. When compared to the CSS approach, it generates 15% and 8% more distillate for depths of 3 cm and 4 cm, respectively. Hence, non-contact structure is sustainable solution for solar desalination.

Keywords: Fouling free, Long Life, Non-contact structure, Solar still, Water depths

1 Introduction

A civilized society relies on energy and potable water for drinking, household tasks, and industrial operations. Urbanization and industrialization increase demand for water, leading to declining groundwater levels and a decline in freshwater levels [1]. In order to achieve equilibrium between supply and demand, the process of desalination is employed to remove salt from saltwater that makes up three-fourths of the planet's surface. This is necessary due to the quantity of seawater and solar energy [2,3]. The issue of water scarcity may have an enticing answer in the form of solar desalination of seawater, despite the lack of access to electricity for desalination. Solar radiations are electromagnetic waves that originate from the sun, passing via the solar glass cover during the solar desalination process. These radiations

* Corresponding Author: ajaykaviti@gmail.com, ajaykumar_k@vnrvjiet.in

change in wavelength when they come into contact with a blackened surface, producing long heatwaves that the basin and liquid contained within the solar still are able to absorb [4,5]. As the water heats up, it begins to evaporate and then forms as droplets on the inner side of the glass lid. The force of gravity drives the condensed liquid to move towards the passageway linked to the solar still short side, where it gets stored in the vessel [6].

Solar stills using phase-change materials (PCM) have potential to improve desalination, as an economic investigation was conducted to assess the yearly output of these materials [7]. It has been discovered that truncated conic fins in solar stills have greater productivity than traditional stills due to truncated conic fins transmitting more heat to the water around them [8]. The combination of evacuated tubes and calcium stones in solar stills yields maximum output throughout the day and night, as calcium stones absorb heat and increase yield during the night [9]. Solar stills with magnets improve internal heat transfer coefficients and output productivity, especially when using saltwater magnetization, by augmenting the static magnetic field [10]. Water-soluble dyes boost the output of deep-basin solar stills. In terms of boosting evaporation and lightfastness, black napthylamine dye is the best choice [11]. Nanoparticles enhance evaporation and output rates in solar stills, resulting in a 25% increase in water output compared to traditional stills due to enhanced heat exchange and water temperature [12]. Water nanofluids of varied concentrations of thermal and physical properties of aluminium oxide (Al_2O_3), zinc oxide (ZnO), iron oxide (Fe_2O_3), and tin oxide (SnO_2) were determined, and the best-suited nanofluids were chosen for performance assessment in a solar still [13]. The employment of distinct aspect ratios with the exact same surface and wick materials, as well as glass cover cooling and external reflectors, to improve wick solar stills performance is dependent on an actual knowledge of the appropriate wick substance varieties and sizes [14]. Nanofluids are being used to boost the efficiency of solar desalination plants [15]. The use of black jute wick belts and graphene nanofluid quantum dots in a solar still significantly enhanced clean water condensate and thermal power efficiency [16]. An integrated carbon dioxide power cycle with geothermal energy provides power for reverse osmosis desalination for freshwater production [17]. Effective solar desalination equipment is made possible by nanostructures with plasma-enhanced resonance, the wave-guide effect, interfacial heat localization, and capillary action [18]. The primary power-consuming component and the amount of electrical energy used in the system are discovered initially through an energy analysis [19]. All these solar desalination improvement approaches studied in contact with water have productivity and fouling capacity limitations. To overcome the constraints of direct contact approaches, a non-contact nanostructure is used. In this work, solar desalination is performed at higher depths (3 cm and 4 cm) for non-contact nanostructure to avoid limitations of fouling.

2 Material fabrication and experimentation

2.1 Development of perforated steel

An SS202 sheet with dimensions of 490 × 490 × 0.8 mm was used, and it contained holes of 2.6 mm in diameter at a distance between centres of 1 cm, with 5% of the sheet left open. The NCNS's exposed top layer receives solar radiation and has holes for water vapor movement, resulting in a 5% open area. Drilling bent the sheet, requiring flattening before

polishing [20]. For applying the solar selective absorber coating, mirror polishing is done on perforated sheet, as shown in Fig. 1.

Fig. 1. Stainless steel sheet after mirror polishing.

2.2 Creation of a perforated sheet with a high absorptive nano coating

From Merck, we obtained sodium dichromate dihydrate ($Na_2Cr_2O_7$), isopropyl alcohol (IPA; 99%), sulfuric acid (98%), and deionized water to create nanocoating on the perforated sheet. A solar selective absorber was created on a reflective mirror-finished SS202 perforated sheet using a controlled chemical oxidation process. A highly absorbent nanocoating was developed using a temperature-controlled chemical bath reactor with 1-M ($Na_2Cr_2O_7$), salt in sulphuric acid and water. Chemical oxidation involves submerging a cleaned perforated sheet in an acid solution for 30 minutes, creating a partially acidic, greyish blue, lustrous nanoporous composite oxide layer. This transforms the sheets into specialized nanocoatings for absorbers. After oxidation, the sheet is cleaned with an environmental fiber cloth and heated in a heating oven for 10 minutes [21]. The digital image of absorptive coating is illustrated in Fig. 2.

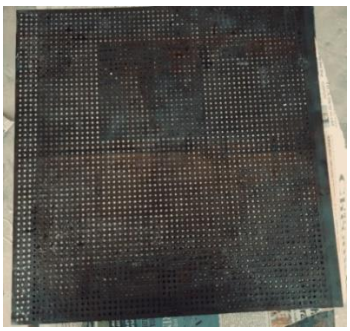

Fig. 2. Digital image of high absorptive coating.

2.3 Creation of a perforated sheet with an emissive coating

The top surface of a non-contact nanostructure (NCNS) needs to be highly absorbent for optimal solar energy absorption, while the bottom surface must be emissive for heat radiation transfer. The challenge lies in achieving an extremely absorbent and extremely emissive side of NCNS, as the absorptive layer may be present on the top. An emissive surface must be

created on the bottom side, then washed with purified water to remove surface impurities. Rust oleum's flat black protective enamel spray was used to create a high emissive surface, with open areas covered with tape and shielding covers removed for final NCNS [22]. The digital image of emissive coating is illustrated in Fig. 3.

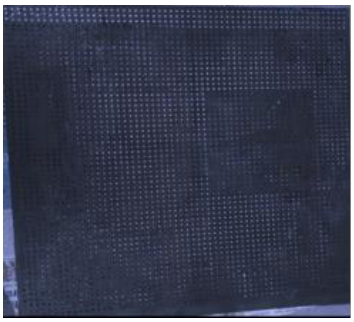

Fig. 3. Digital image of high emissive coating.

2.4 Experimental setup and procedure

The single-slope NCNS external assembly was constructed with a two-inch-thick plyboard. The dimensions of the exterior wooden assembly's basin were 53.8 x 53.8 cm. The front side was 20 cm tall, while the back was 37 cm tall. The exterior component was constructed to prevent thermal dissipation into the surroundings and to isolate the flow of heat. The outside part serves to isolate the heat flow and was built to prevent temperature loss to the environment. The NCNS internal assembly was constructed using a 1mm dense GI. The maximum insolation-capable sink surface area was 2500cm², which has a black powder coating on it. The rear side's elevation is 35 cm, whereas the shorter side measures 18.8 cm. At the back of the SS, a 0.635 mm diameter galvanized pipe was welded to allow saltwater to enter and exit [22]. The short side is to attach the 52 x 54 x 0.4 cm glass cover to the SS assembly's apex. Using acrylic rods with a 4.5 cm height, the NCNS and sink liner's heights were adjusted. Kapton tape was used to cover the NCNS's edges, which are 0.12 W/m-k thermally conductive. Dual-sided tape was applied to the top edges, and silicon sealant was applied to the gap between the glass and tape. A semi-circular channel was connected to the SS's small side to collect condensed distilled water. This process ensures a robustly sealed solar still, preventing water vapor from escaping [23].

To avoid the NCNS making thermal contact with the solar still's walls, after completion of the setup, we first need to connect the sensors to the systems to know the various temperatures by using thermocouples. The thermocouples are connected to the data acquisition system for measuring temperatures. Sunlight intensity can be measured with the help of a pyranometer. For 4cm depth, 10 litres of water are poured in a still for experimentation; for 3cm depth, 8.75 litres of water are poured in both conventional and non-contact nanostructure stills. The pyranometer instrument is utilized to measure sun irradiance and ambient temperature, and a data acquisition system is used. The experimentation starts at 9 a.m. and goes on until 5 p.m. The readings of the temperatures are taken every half an hour, as are the readings of the distillate produced. The readings of the NCNS system and CSS system are noted for comparison. The image of a non-contact nanostructure solar still (NCNS system) and a conventional solar still system (CSS system) is illustrated in Fig. 4.

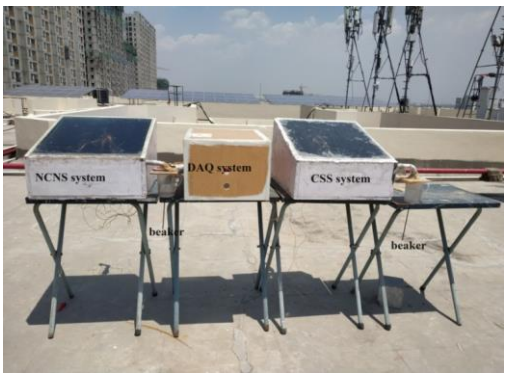

Fig. 4. Image of NCNS and CSS system.

3 Results and discussions

3.1 Technical analysis

The trials were carried out using tap water over a span of three distinct months: June (2023), August (2023), and October (2023), with different depths of water such as 3cm and 4cm. The experiments for the NCNS system and the CSS system were conducted simultaneously. Fig. 5 shows the relationship between solar intensity and time. On June 12, 2023, at 12:00 pm, a sun intensity of 1020 W/m^2 was recorded, reaching its highest point. This intensity was measured for a water depth of 3cm, and on August 24, 2023, at 2:00 pm, a solar intensity of 988 W/m^2 was recorded, reaching its highest point. This measurement was taken at a depth of 4cm of water.

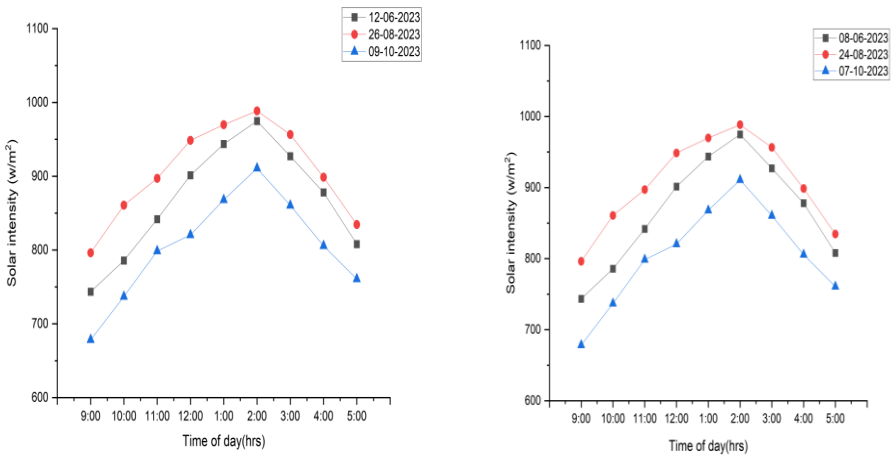

(a) (b)

Fig. 5. a) Variations of solar intensity vs time (a) for 3cm depth of water (b) for 4cm depth of water.

Fig. 6 shows the variation of ambient temperature vs time. The highest recorded ambient temperature of 42ºC occurred on June 12th at 3p.m. at a water depth of 3cm. and the highest recorded ambient temperature of 45ºC occurred on august 24th at 2p.m. at a water depth of 4cm.

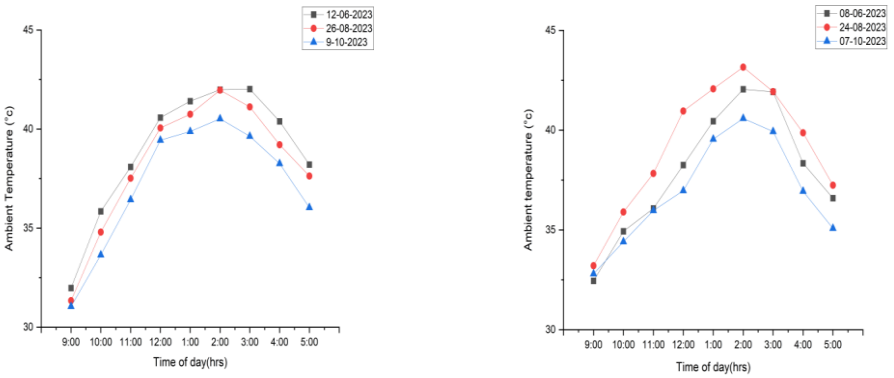

(a) (b)

Fig. 6. a) Variations of Ambient temperature vs time (a) for 3cm depth of water (b) for 4cm depth of water.

Fig. 7 shows the fluctuations of still temperatures vs time for a 3cm depth of water at three different months. Fig. 8 shows the fluctuations of still temperatures vs time for a 4cm depth of water at three different months of the NCNS system. In all cases, absorber temperature is higher at 2 p.m. because there is the highest solar intensity. The absorber typically consists of a substance with a high solar absorptance.This implies that it has the ability to effectively capture solar light and transform it into thermal energy. The absorber is specifically engineered to efficiently capture sunlight, leading to its subsequent thermal elevation. Elevated temperatures are crucial for desalination, which involves water vaporization. The lowest temperature is the basin temperature. When heated, infrared radiation (IR) is consumed by the uppermost layer of water, selectively warming it. Convection and conduction transfer heat from the lower water layer to the basin liner, resulting in a warming effect. It follows the same trend of temperatures for both depths of water.

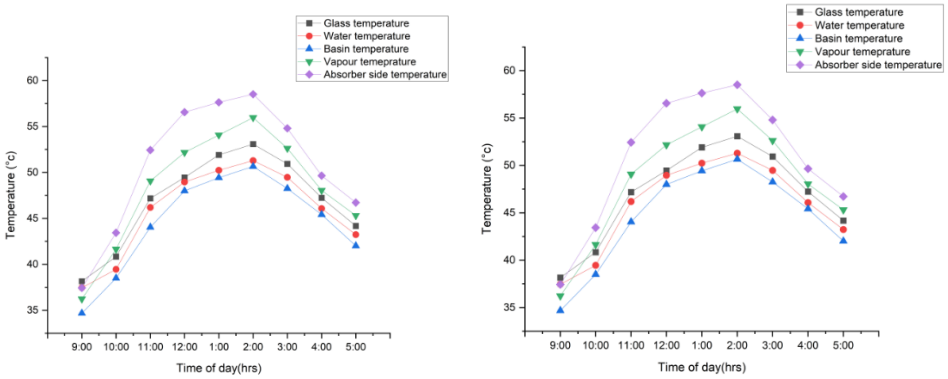

(a) (b)

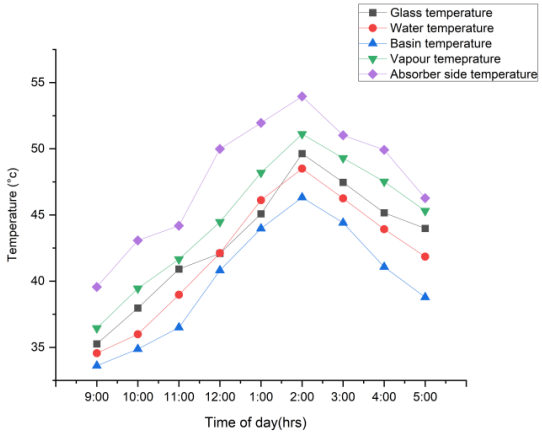

(c)

Fig. 7. Variations of still temperatures vs time of NCNS system for 3cm depth of water (a) on 12-06-2023 (b) on 26-08-2023 (c) on 09-10-2023.

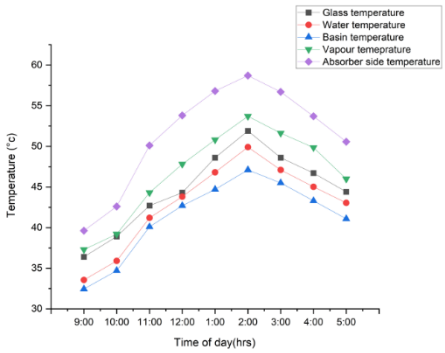

(a)

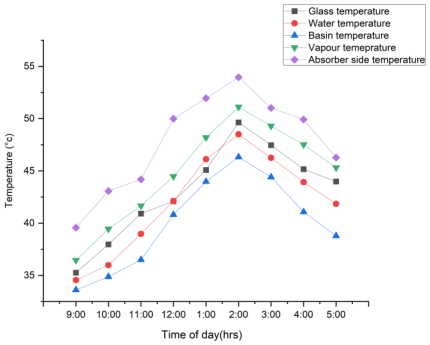

(b)

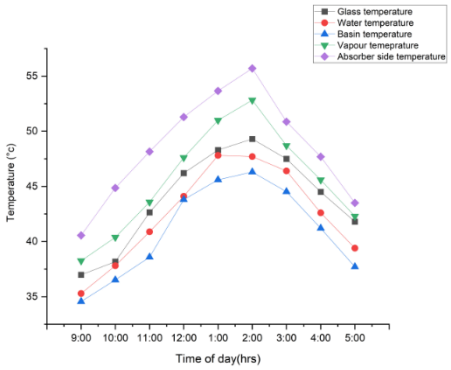

(c)

Fig. 8. Variations of still temperatures vs time of NCNS system for 4cm depth of water (a) on 08-6-2023 (b) on 24-8-2023 (c) on 07-10-2023.

Fig. 9 shows the fluctuations of still temperatures vs time for a 3cm depth of water at three different months, and Fig. 10 shows the fluctuations of still temperatures vs time for a 4cm depth of water at three different months of the CSS system. Basin temperature is the highest temperature in this system during 2 p.m., and glass temperature is the lowest temperature among all temperatures because the basin water in a CSS system exhibits significant thermal inertia. This leads to a delay in attaining the highest water temperature and, consequently, the temperature of the glass cover.

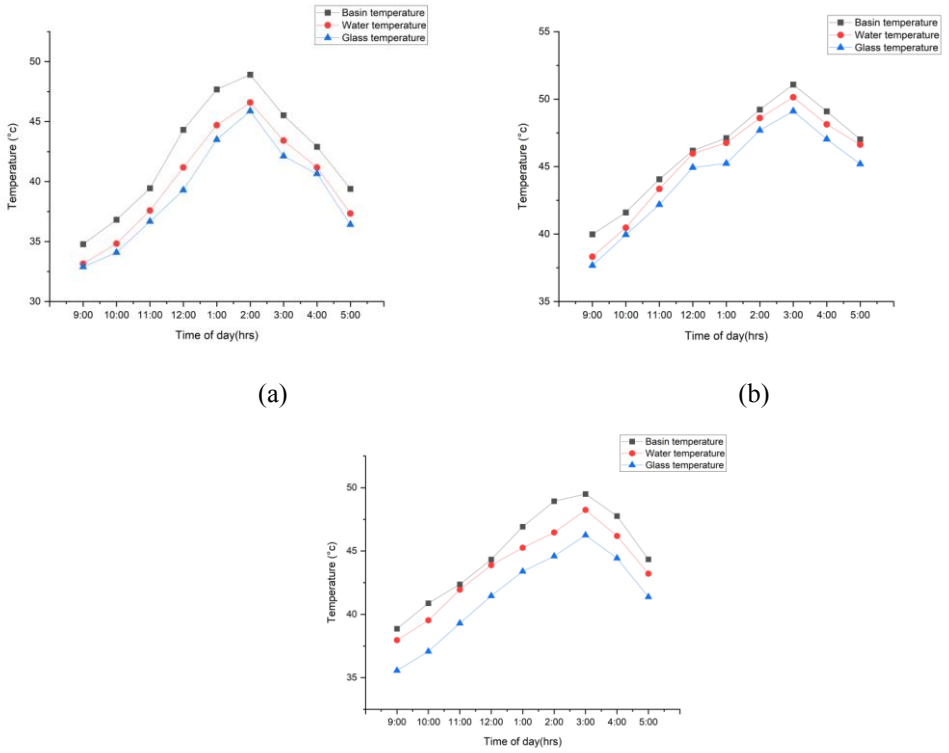

(a) (b)

(c)

Fig. 9 Variations of still temperatures vs time of CSS system for 3cm depth of water (a) on 12-06-2023 (b) on 26-8-2023 (c) on 09-10-2023.

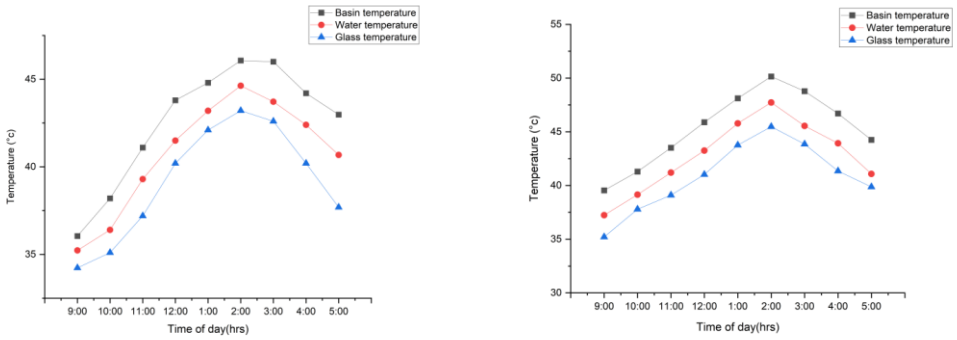

(a) (b)

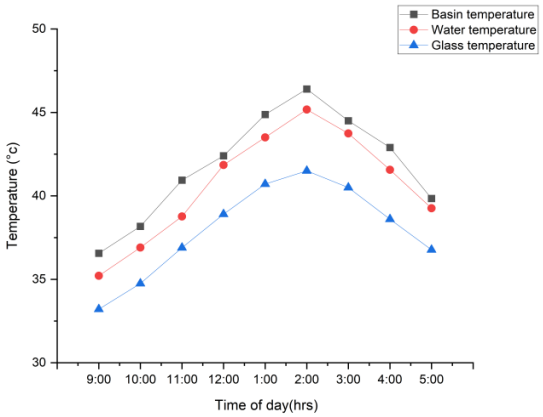

(c)

Fig. 10 Variations of still temperatures vs time of CSS system for 4cm depth of water (a) on 08-6-2023 (b) on 24-8-2023 (c) on 07-10-2023.

Fig. 11 shows the variations of distillate vs time for a 3cm depth of water at three different months for the NCNS system and CSS system. The highest production of distillate was recorded on 12-06-2023 for both systems. Maximum distillate production rate was recorded from 1 p.m. to 3 p.m. because of higher solar intensity.

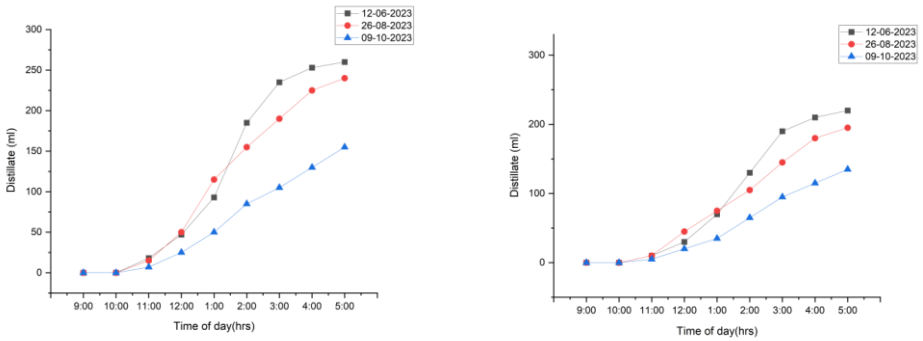

(a) (b)

Fig. 11 Variations in the distillate versus time for 3cm depth of water of (a) NCNS system (b) CSS system.

Fig. 12 shows the distillate production variations for 4cm depth of water in NCNS and CSS systems at different months. The highest production was recorded on 24-08-2023, with maximum production rates from 1 p.m. to 3 p.m., due to higher solar intensity. Non-contact nano structure system produces higher distillate at 3cm and 4cm depths. For 3cm and 4cm depth, it achieves 15% and 8% higher distillate than the CSS system.

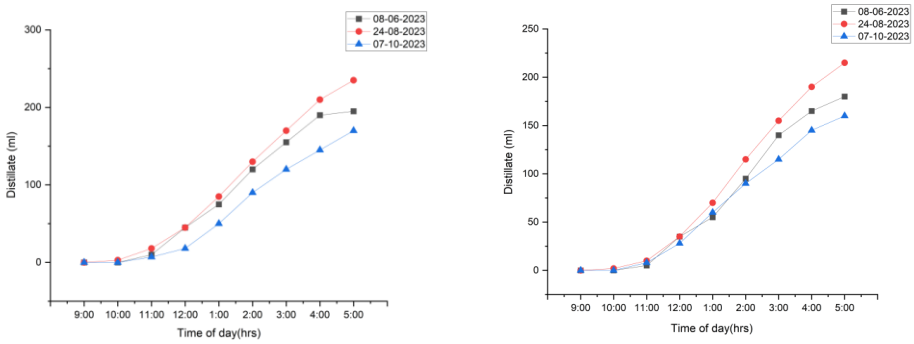

Fig. 12 Variations in the distillate versus time for 4cm depth of water of (a) NCNS system (b) CSS system.

4 Conclusions

Experiments were conducted using saline water at 3cm and 4cm depths. The data was collected over three different months to check efficacy of the structure in different conditions of the environment. The experimental data comprised of many parameters, such as temperatures of glass, basin, vapor, water, absorber, ambient temperature, time, and solar intensity are measured during the experimentation. The following on the salient findings.

- Non-contact nanostructure solar still produces more distillate from 2 p.m. to 5 p.m. in comparison with conventional solar still.
- At higher depths non-contact nano structure giving higher distillate than the conventional desalination system.
- For 3cm and 4cm depths, it achieves 15% and 8% higher distillate than the conventional solar desalination system.

References

1. F. A. Raihananda *et al.*, “Low-cost floating solar still for developing countries: Prototyping and heat-mass transfer analysis,” *Results Eng.*, vol. 12, p. 100300, 2021, doi: 10.1016/j.rineng.2021.100300.
2. Z. Xu *et al.*, “Ultrahigh-efficiency desalination: Via a thermally-localized multistage solar still,” *Energy Environ. Sci.*, vol. 13, no. 3, pp. 830–839, 2020, doi: 10.1039/c9ee04122b.
3. F. E. Ahmed, R. Hashaikeh, and N. Hilal, “Solar powered desalination – Technology, energy and future outlook,” *Desalination*, vol. 453, no. November 2018, pp. 54–76, 2019, doi: 10.1016/j.desal.2018.12.002.
4. K. Selvaraj and A. Natarajan, “Factors influencing the performance and productivity of solar stills - A review,” *Desalination*, vol. 435. Elsevier B.V., pp. 181–187, Jun. 01, 2018. doi: 10.1016/j.desal.2017.09.031.
5. A. K. Kaviti, A. Yadav, and A. Shukla, “Experimental investigation of solar still with opaque north triangular face,” *Int. J. Green Energy*, vol. 16, no. 6, pp. 442–449, 2019, doi: 10.1080/15435075.2019.1578658.

6. Akkala, Siva Ram, and Ajay Kumar Kaviti. "Advanced design techniques in passive and active tubular solar stills: a review." *Environmental Science and Pollution Research* 29, no. 32 (2022): 48020-48056. https://doi.org/10.1007/s11356-022-20664-6
7. Y. Le Nian, Y. K. Huo, and W. L. Cheng, "Study on annual performance of the solar still using shape-stabilized phase change materials with economic analysis," *Sol. Energy Mater. Sol. Cells*, vol. 230, no. January, p. 111263, 2021, doi: 10.1016/j.solmat.2021.111263.
8. A. K. Kaviti, V. R. Naike, A. S. Ram, S. Hussain, and A. A. Kumari, "Energy and exergy analysis of double slope solar still with aluminium truncated conic fins," *Mater. Today Proc.*, vol. 45, no. xxxx, pp. 5387–5394, 2021, doi: 10.1016/j.matpr.2021.02.047.
9. H. Panchal, S. S. Hishan, R. Rahim, and K. K. Sadasivuni, "Solar still with evacuated tubes and calcium stones to enhance the yield: An experimental investigation," *Process Saf. Environ. Prot.*, vol. 142, pp. 150–155, 2020, doi: 10.1016/j.psep.2020.06.023.
10. A. K. Kaviti, A. S. Ram, and A. K. Thakur, "Influence of fully submerged permanent magnets in the evaluation of heat transfer and performance analysis of single slope glass solar still," *Proc. Inst. Mech. Eng. Part A J. Power Energy*, vol. 236, no. 1, pp. 109–123, 2022, doi: 10.1177/09576509211031021.
11. A. K. Rajvanshi, "Effect of various dyes on solar distillation," *Sol. Energy*, vol. 27, no. 1, pp. 51–65, 1981, doi: 10.1016/0038-092X(81)90020-7.
12. A. E. Kabeel, Z. M. Omara, F. A. Essa, A. S. Abdullah, T. Arunkumar, and R. Sathyamurthy, "Augmentation of a solar still distillate yield via absorber plate coated with black nanoparticles," *Alexandria Eng. J.*, vol. 56, no. 4, pp. 433–438, 2017, doi: 10.1016/j.aej.2017.08.014.
13. T. Elango, A. Kannan, and K. Kalidasa Murugavel, "Performance study on single basin single slope solar still with different water nanofluids," *Desalination*, vol. 360, pp. 45–51, 2015, doi: 10.1016/j.desal.2015.01.004.
14. S. W. Sharshir, M. Salman, S. M. El-Behery, M. A. Halim, and G. B. Abdelaziz, "Enhancement of solar still performance via wet wick, different aspect ratios, cover cooling, and reflectors," *Int. J. Energy Environ. Eng.*, vol. 12, no. 3, pp. 517–530, 2021, doi: 10.1007/s40095-021-00386-0.
15. S. R. Akkala, A. K. Kaviti, T. ArunKumar, and V. S. Sikarwar, "Progress on suspended nanostructured engineering materials powered solar distillation- a review," *Renew. Sustain. Energy Rev.*, vol. 143, no. June 2020, p. 110848, 2021, doi: 10.1016/j.rser.2021.110848.
16. F. A. Essa, Z. M. Omara, A. S. Abdullah, A. E. Kabeel, and G. B. Abdelaziz, "Enhancing the solar still performance via rotating wick belt and quantum dots nanofluid," *Case Stud. Therm. Eng.*, vol. 27, no. July, p. 101222, 2021, doi: 10.1016/j.csite.2021.101222.
17. S. Hoseinzadeh, R. Yargholi, H. Kariman, and P. S. Heyns, "Exergoeconomic analysis and optimization of reverse osmosis desalination integrated with geothermal energy," *Environ. Prog. Sustain. Energy*, vol. 39, no. 5, 2020, doi: 10.1002/ep.13405.
18. S. A. Mohiuddin, A. K. Kaviti, and T. Srinivasa Rao, *Nanostructures as High Absorption Energy Materials—A Review*. Springer Singapore, 2021. doi: 10.1007/978-981-16-0976-3_30.
19. H. Kariman, S. Hoseinzadeh, and P. S. Heyns, "Energetic and exergetic analysis of evaporation desalination system integrated with mechanical vapor recompression circulation," *Case Stud. Therm. Eng.*, vol. 16, p. 100548, 2019, doi: 10.1016/j.csite.2019.100548.
20. S. A. Mohiuddin, A. K. Kaviti, T. S. Rao, and S. Sakthivel, "Effect of water depth in productivity enhancement of fouling-free non-contact nanostructure desalination

system," *Sustain. Energy Technol. Assessments*, vol. 54, no. June, p. 102848, 2022, doi: 10.1016/j.seta.2022.102848.

21. S. A. Mohiuddin, A. K. Kaviti, T. S. Rao, and S. R. Atchuta, "Effect of air gap in novel fouling-free non-contact nanostructure solar still for potable water application from lake water," *J. Clean. Prod.*, vol. 381, no. P1, p. 135100, 2022, doi: 10.1016/j.jclepro.2022.135100.
22. S. Afzal Mohiuddin *et al.*, "Performance analysis of non-contact nanostructure solar desalination system by varying water depth at a constant air gap," *Sol. Energy*, vol. 247, no. October, pp. 485–498, 2022, doi: 10.1016/j.solener.2022.10.042.
23. S. A. Mohiuddin, A. K. Kaviti, T. S. Rao, and S. Sakthivel, "Performance analysis of a contactless nanostructure in solar-powered desalination system," *Environ. Sci. Pollut. Res.*, vol. 30, no. 6, pp. 16277–16288, 2023, doi: 10.1007/s11356-022-23130-5.